Vol. 23, No. 5

BRCT Domain-Containing Protein PTIP Is Essential for Progression through Mitosis

Eun Ah Cho,[1] Marc J. Prindle,[2] and Gregory R. Dressler[1]*

*Department of Pathology[1] and Program in Cell and Molecular Biology,[2]
University of Michigan, Ann Arbor, Michigan 48109*

The Pax transactivation domain-interacting protein (PTIP) is a large nuclear protein with multiple BRCT domains that was identified on the basis of its interaction with transcription factors of the Pax and Smad families. To address the function of PTIP during mouse development, we generated a constitutive null allele. Homozygous *PTIP* mutants are developmentally retarded, disorganized, and embryonic lethal by day 9.5 of embryonic development (E9.5). *PTIP* mutant cells appear to replicate DNA but show reduced levels of mitosis and widespread cell death by E8.5. DNA damage appears to precede nuclear condensation at E7.5, suggesting a defect in DNA repair. Neither embryonic fibroblast nor embryonic stem cells from *PTIP* mutants proliferate in culture, suggesting a fundamental defect in cell proliferation. Trophoblast cells from *PTIP* mutants are more sensitive to DNA-damaging agents. Condensation of chromatin and expression of phospho-histone H3 are also affected in *PTIP* mutants, and this may underlie the inability of *PTIP* mutants to progress through mitosis. Given the role of BRCT domain proteins in DNA repair and cell cycle control, we propose that PTIP is an essential element of the cell proliferation machinery, perhaps by functioning in the DNA repair pathways.

Murine PTIP (Pax transactivation domain-interacting protein) was identified on the basis of its interaction with the Pax family of DNA binding transcription factors (13). PTIP is a large nuclear protein with multiple BRCT domains. The BRCT domain was originally described in the carboxy terminus of the BRCA1 tumor suppressor protein (12), yet hydrophobic cluster analysis revealed a large family of nuclear proteins, across divergent species, with similar BRCT repeats. Like *BRCA1*, many of these genes are thought to function in regulation of the cell cycle, in activation of cell cycle checkpoints, and/or in mediation of responses to DNA-damaging agents. For example, BRCA1 activates the G_2/M checkpoint, in response to DNA damage, through the Chk1 kinase (24). The BRCT domains are essential for BRCA1 activity, as both human mutations and targeted mouse mutations have demonstrated (8). In yeast, the BRCT domain protein Cut5/Rad4 interacts with a second BRCT domain protein, Crb2, to activate the DNA damage checkpoint (18). Phosphorylation of Crb2 by cdc2/CDK1 is necessary for re-entry into mitosis after DNA repair (5) and for topoisomerase III function in recombination-mediated repair (2).

In addition to their potential roles in DNA repair pathways, the nuclear BRCT domain proteins have also been linked to gene activation (22). In *Xenopus laevis*, the PTIP-related protein Swift was identified on the basis of its ability to bind the Smad2 transcription factor and accentuate Smad2-dependent transcription (20). At the time of gastrulation, Smad2 mediates gene activation in response to signaling by the secreted transforming growth factor β family member Activin. PTIP also interacts with the Pax family of transcription regulators (13) and, at least in one case, is able to inhibit transactivation of the

glucagon promoter in pancreatic cells (7). PTIP and Swift contain two amino-terminal BRCT domains, a glutamine-rich region, and three and four carboxy-terminal BRCT domains, respectively.

In order to discern the role of PTIP in development, we generated a null allele in mice by homologous recombination. *PTIP* mutants show greatly enhanced cell death prior to and at the time of gastrulation and were severely retarded thereafter. In *PTIP*-null mutants, cells replicate DNA but exhibit DNA damage, as evidenced by the terminal deoxynucleotidyltransferase-mediated dUTP-biotin nick end labeling (TUNEL) assay. Embryonic fibroblasts or inner cell mass cells fail to grow out from *PTIP*-null embryos in vitro. In *PTIP* mutants, cells exhibit suppressed levels of phospho-histone H3, which is required for proper chromatin condensation. In cells entering mitosis, chromatin condensation appears to be affected, with few well-demarcated chromosomes evident. By day 8.5 of embryonic development (E8.5), few cells are seen in mitosis. The data imply that PTIP has an essential role in cell division after S phase and before completion of mitosis.

MATERIALS AND METHODS

Generation of a *PTIP*-null allele. The targeting vector was linearized with *Not*I, and 80 μg of DNA was electroporated into 32×10^6 R1 ES cells (129/SVJ). ES cell colonies with recombined DNA were selected with 300 μg of G418 per ml and 2 μM ganciclovir as previously described (11). Approximately 500 resistant ES cell clones were screened by Southern blotting with probes corresponding to the 5′ and 3′ sequences of the targeted region. Approximately 30 positive clones were identified, and 4 of these were karyotyped for the correct number of mouse chromosomes. Three cell lines were used for injection into recipient C57BL/6 blastocysts, and chimeric mice were identified by coat color. Chimeric males were bred for germ line transmission, and agouti offspring were genotyped for the *PTIP* mutation by Southern blotting. Heterozygous crosses were then set up to generate homozygous *PTIP* mutants. For better breeding and embryo collection, the genetic background of *PTIP* mutant mice was kept at approximately 50% 129SVJ and 50% C57BL/6.

BrdU labeling and TUNEL assay. Pregnant female mice were injected intraperitoneally with bromodeoxyuridine (BrdU; Sigma) in phosphate-buffered sa-

* Corresponding author. Mailing address: 1150 W. Medical Center Dr., Ann Arbor, MI 48109-0650. Phone: (734) 764-6490. Fax: (734) 763-6640. E-mail: Dressler@umich.edu.
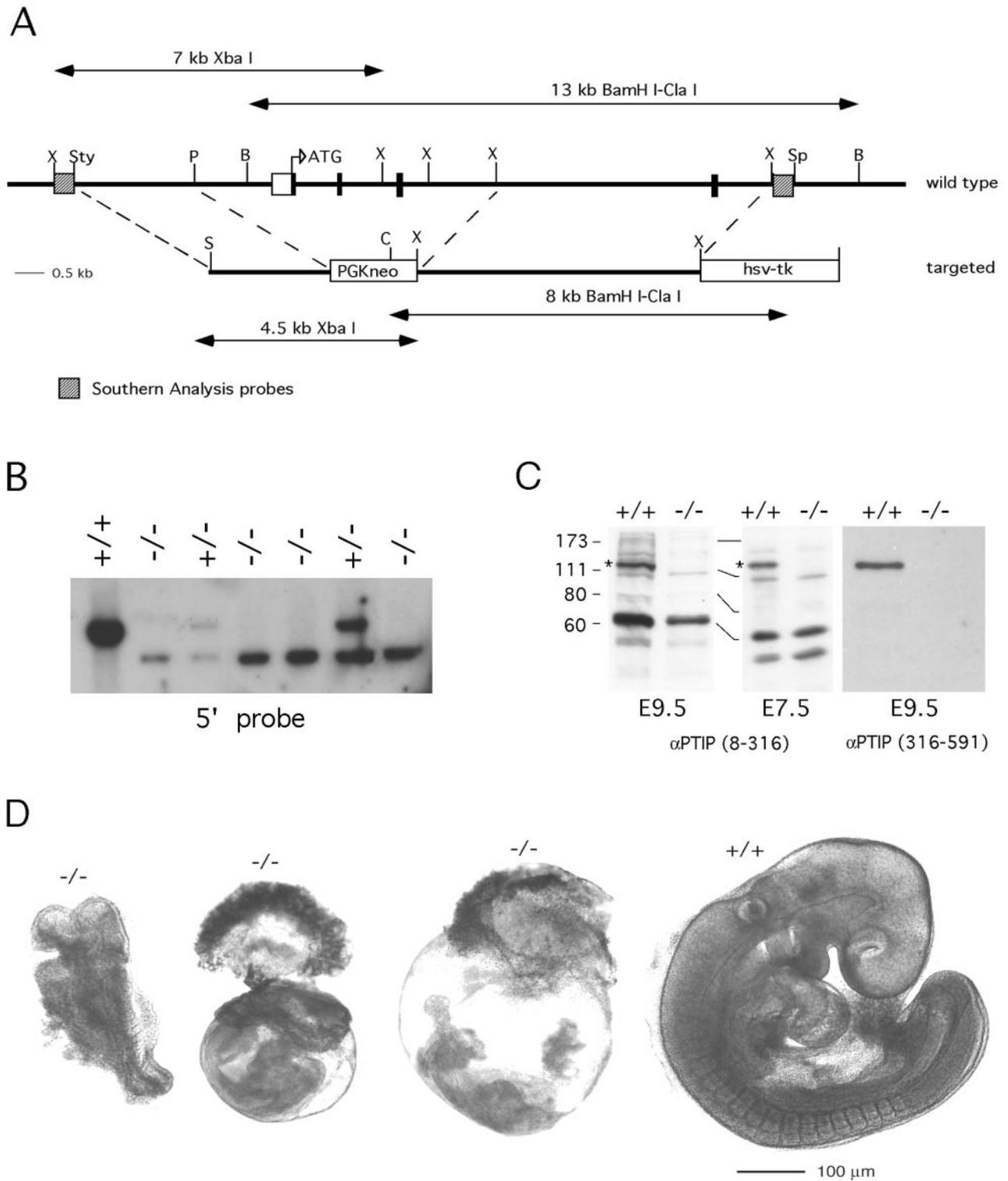
FIG. 1. Generation of a *PTIP*-targeted allele by homologous recombination. (A) The gene-targeting vector contained 2.2 kb of 5′-flanking sequence, the PGKneo cassette, a 3′ flank of 5.8 kb, and the herpes simplex virus thymidine kinase (hsv-tk) gene for negative selection. (B) Southern blot of *Xba*I-digested E9.5 mouse DNA probed with the 5′ probe outside of the targeting vector. The *PTIP* genotypes are indicated. (C) Western blots of total protein lysates from E9.5 and E7.5 embryos. Blots were probed with antibodies against either PTIP amino acids 8 to 316 or 316 to 591, as indicated. The asterisks indicates the position of full-length PTIP. (D) Wild-type (+/+) and *PTIP* mutant embryos collected at E9.5. The mutant on the left is dissected free of extraembryonic membranes. Note the size and disorganization of the *PTIP* mutants relative to wild-type embryos.
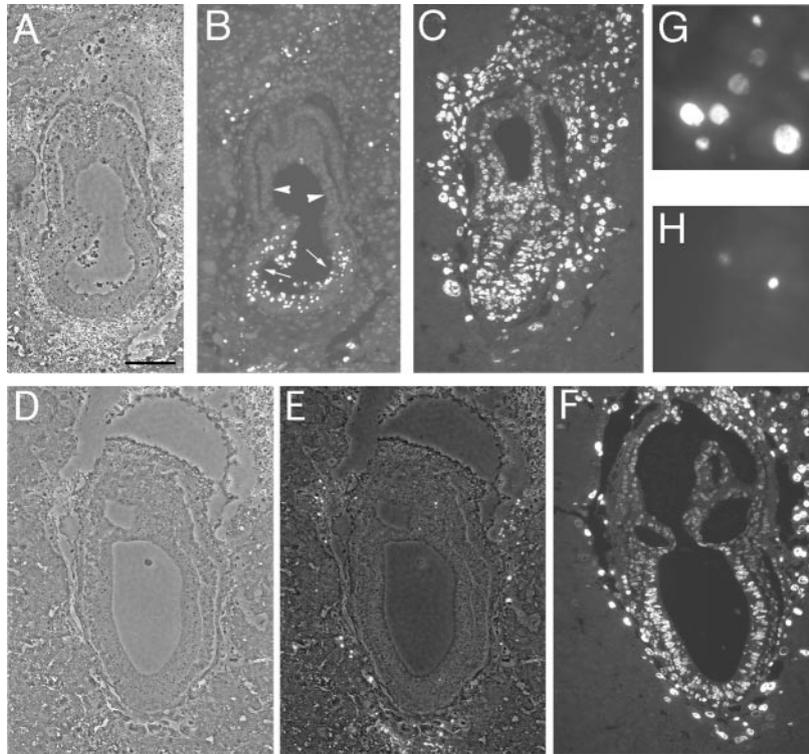
FIG. 2. Cell proliferation and cell death at E7.5. Pregnant females were injected with BrdU (3 mg/100 g of body mass), and embryos were harvested after 2 h. $PTIP^{-/-}$ mutant sections (A to C) and wild-type littermate sections (D to F) stained with the TUNEL reaction (B and E) or with anti-BrdU (C and F) are shown. The bar in panel A is 100 μm for panels A to F. Note the appearance of TUNEL-positive cells within the embryonic ectoderm of $PTIP$ mutants (arrows, B) but not in the extraembryonic part of the egg cylinder (arrowhead, B). BrdU-positive cells were dispersed throughout the $PTIP$-null and wild-type embryos at this stage. (G) High magnification of TUNEL-positive nuclei form a $PTIP$-null mutant shows labeling of nuclei before nuclear condensation has occurred. (H) TUNEL-positive nuclei of wild-type embryos were almost always pyknotic.

line (PBS) at a concentration of 3 mg/100 g of body mass. Mice were sacrificed after 2 or 4 h. Embryos were fixed overnight in paraformaldehyde, dehydrated, and embedded in paraffin. Sections were cut at 8 μm, deparaffinized, rehydrated, and permeabilized with 2 N HCl–0.5% Triton X-100–PBS for 10 min. Anti-BrdU (Sigma) was diluted 1:100 in PBS–0.5% Tween 20 (PBST) containing 2% goat serum and incubated for 1 h at room temperature. Slides were washed three times in PBST and incubated with fluorescein isothiocyanate (FITC)-conjugated anti-mouse antibodies (Sigma) for 1 h. Slides were washed three times in PBST and mounted with Gelvatol. The TUNEL reaction was performed with the FITC-labeled Apotag kit (Boehringer Mannheim, Inc.) in accordance with the manufacturer's protocol, except that the permeabilization time was increased to 20 min.

Protein analysis. Embryos were dissected free from the yolk sac, which was saved for DNA extraction, and lysed in 100 ml of PK lysis buffer (50 mM HEPES [pH 7.5], 150 mM NaCl, 1.5 mM MgCl₂, 1 mM EGTA, 10% glycerol, 1% Triton X-100, 1 mM Na vanadate, 50 mM NaF, 500 nM okadaic acid, 1× protease inhibitor cocktail [Roche]). Approximately 20 μg of total protein was boiled in 1× sodium dodecyl sulfate-polyacrylamide gel electrophoresis (SDS-PAGE) buffer and subjected to SDS–10% PAGE. After transfer to polyvinylidene fluoride membrane, membranes were blocked with 5% milk in TBS and incubated for 3 h with 1 μg of antibodies against P-histone H3 or acetyl-histone H3 (Upstate Biotech) per ml in 1× TBS–1% milk–0.1% Tween 20 (TBSTM). Membranes were washed three times for 15 min (each time) in TBSTM and incubated with horseradish peroxidase-conjugated anti-mouse antibodies (Amersham Inc.). Membranes were washed three times in TBSTM and two times in TBS for 15 min (each time) and visualized by chemiluminescence in accordance with the manufacturer's (NEN) protocol.

Cell cycle expression. To determine the expression profile of PTIP during the cell cycle, we utilized both NIH 3T3 cells and wild-type primary mouse embryo fibroblasts (MEFs). Cells were plated at $5 \times 10^5/60$-mm-diameter plate and serum starved for 48 h in Dulbecco modified Eagle medium (DMEM) with 0.5% fetal calf serum. Quiescent cells were then activated with either 10% fetal calf serum, for NIH 3T3 cells, or 20% fetal calf serum, for MEFs. At various time

points after serum addition, cells were rinsed in PBS and scraped. Equal numbers of cells were lysed in PK lysis buffer, and proteins were analyzed by SDS-PAGE and Western blotting.

Blastocyst outgrowths. Four- to 5-week-old females were injected with 5 IU of pregnant mare serum gonadotropin and 2 days later with 5 IU of human chorionic gonadotropin. The blastocysts were flushed out of the uterine horns 3 days after vaginal plug detection. Blastocysts were cultured on gelatinized 96-well round-bottom plates in DMEMD supplemented with 20% fetal calf serum. For radiation sensitivity assays, blastocysts were exposed to 2 Gy of ionizing radiation at day 0 and cultured for 7 days. Cells were stained with Hoechst fluorescent dye and counted.

Immunostaining. E7.5 and E8.5 embryos were dissected free of the decidua, and a small piece of the amniotic membrane was used to genotype the mutants by PCR using primers specific for the *neo* cassette and primers specific for the wild-type *PTIP* allele. Embryos were fixed in 4% paraformaldehyde–PBS at 4°C, dehydrated in graded ethanol, and embedded in paraffin. Sections were cut at 3 to 4 μm. After dewaxing and rehydration, sections were boiled for 8 min in a pressure cooker with a 1:100 dilution of antigen unmasking solution (Vector Laboratories). Sections were washed in PBS and incubated with antibodies against P-histone H3 (Upstate Biotech), α-tubulin (Sigma), or γ-tubulin (Sigma) in a buffer consisting of PBS, 0.1% Tween 20, and 2% goat serum. After incubation for 2 h at room temperature, sections were washed two times for 10 min (each time) in PBS–0.1% Tween 20 and incubated with FITC- or tetramethyl rhodamine isothiocyanate-conjugated secondary antibodies for 1 h. Sections were washed two times and covered with Gelvatol containing 0.2% 1,4-diazabicyclo(2,2,2)octane. Photomicrographs were taken with a Nikon ES800 fluorescent micrograph and a Spot digital camera.

RESULTS

In order to better define the role of PTIP in mammalian development, a targeted allele was generated as outlined in
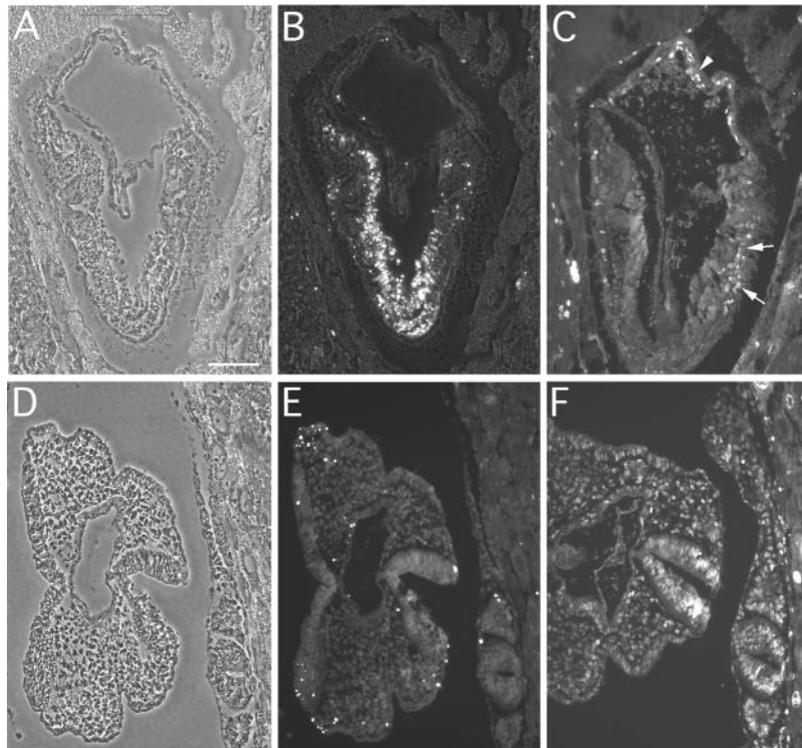
FIG. 3. Cell proliferation and cell death at E8.5. $PTIP^{-/-}$ sections (A to C) and wild-type littermate sections (D to F) stained with the TUNEL reaction (B and E) or with anti-BrdU (C and F) are shown. Note the massive cell death within the *PTIP*-null embryo (B). Incorporation of BrdU at this stage in *PTIP* mutants is found only in regions that show less TUNEL staining (arrows, C) or in the amniotic membrane (arrowhead, C). The bar in panel A is 100 μm for all panels.

Fig. 1A. The gene-targeting vector contained 2.2 kb of 5′-flanking sequence, the PGKneo cassette, a 3′ flank of 5.8 kb, and the herpes simplex virus thymidine kinase gene for negative selection. Homologous recombination would delete exons 1 to 3 of the PTIP coding region, spanning amino acids 1 to 73, and would potentially inhibit expression of downstream sequences. More than 20 independent ES cell clones were identified that had correct homologous recombination, as determined by 5′ and 3′ probes. After karyotyping, four lines were injected into blastocysts to generate chimeric mice. Upon breeding of chimeric males, germ line transmission was achieved with three independently derived chimeras. Heterozygous $PTIP^{+/-}$ mice were generally healthy and indistinguishable from wild-type littermates. Heterozygous *PTIP* mutant mice were bred to generate homozygotes carrying the targeted allele. Initially, offspring from heterozygous crosses were allowed to go to weaning, at which time genotyping was performed. Upon examination of more than 200 litters from two $PTIP^{+/-}$ strains that were derived from different ES cell clones, not a single homozygous *PTIP* mutant mouse was evident. Since there were few deaths from birth to weaning, we concluded that the targeted *PTIP* allele was homozygous embryonic lethal.

Embryos from *PTIP* heterozygous crosses were examined at various times during gestation for evidence of embryonic lethality and genotyped by Southern blotting (Fig. 1B). In addition, pooled lysates from E7.5 and E9.5 embryos were assayed for expression of PTIP (Fig. 1C). Two different chicken anti-

PTIP antibodies were used to detect the 130-kDa full-length PTIP. The more N-terminal antibodies cross-react with additional proteins whose levels were unchanged and provide a convenient control for protein levels. The antibodies against PTIP amino acids 316 to 591 are more specific and do not detect any proteins in the $PTIP^{-/-}$ lysates (Fig. 1C). These data confirm that any expression of coding regions downstream of the targeted exons is severely compromised. At E9.5, gross examination of embryos revealed that *PTIP* homozygous null embryos were developmentally arrested and severely disorganized (Fig. 1D). At this stage, the wild type and heterozygotes exhibited 15 to 20 somites; defined fore-, mid-, and hindbrain regions; a beating heart; well-developed optic and otic vesicles; and forelimb buds. In contrast, the $PTIP^{-/-}$ mutants were significantly smaller, appearing more like disorganized E8.5 embryos. $PTIP^{-/-}$ mutants showed no sign of heart development, little vascularization of the yolk sac, and a poorly defined body axis. The head folds and neural tube were evident in most cases. Occasional somites were discernible, often unilaterally. The allantois had not reached the placenta in mutant embryos.

The size and condition of *PTIP* mutant embryos indicated a lack of proliferation or enhanced cell death. To further characterize the phenotype of *PTIP* mutants, embryos were examined at E7.5 and E8.5 for cell proliferation and apoptosis. Prior to sacrifice of the female, BrdU was injected intraperitoneally to label dividing cells. Embryos were embedded in paraffin and sectioned for histology, for immunostaining with anti-BrdU antibodies, and for cell death staining by the TUNEL assay. At

E7.5 (Fig. 2), $PTIP^{-/-}$ embryos were usually discernible on the basis of their smaller phenotype. While normal embryos had three well-defined cavities, the amniotic, the exocoelomic, and the ectoplacental, $PTIP$-null mutants lacked a clearly defined amnion (Fig. 2A). The ectoplacental cone was well developed in $PTIP$-null embryos, but the egg cylinder was about half as long as that of a normal E7.5 embryo. $PTIP$-null embryos exhibited BrdU incorporation at levels equal to that of the wild type, indicating that cell cycle progression occurred at least to S phase (Fig. 2C and F). BrdU-positive cells were counted and compared to the total number of nuclei observed on given sections. On average, about $63\% \pm 7\%$ of the cells within the embryonic ectoderm were positive for anti-BrdU staining in the wild type or $PTIP$ mutants at E7.5. However, TUNEL staining for apoptosis revealed differences between normal embryos and $PTIP$-null mutants (Fig. 2B and E). $PTIP$ mutants showed significant cell death, particularly within the embryonic ectodermal layer. Strikingly, the extraembryonic and ectoplacental tissues did not exhibit much apoptosis at this stage. Wild-type embryos showed little apoptosis at E7.5, except in the uterine wall. While the TUNEL assay is generally used to mark apoptotic cells, it is really a measure of free DNA ends. During normal apoptosis, nuclear condensation and DNA fragmentation are closely linked. Strikingly, many $PTIP$-null nuclei stained positive in the TUNEL assay even before nuclear condensation was evident, whereas wild-type TUNEL-positive nuclei were almost always pyknotic (Fig. 2G and H). At E8.5, $PTIP$-null embryos were developmentally arrested and disorganized (Fig. 3A and D). Neural plate and mesodermal tissues could be identified morphologically, indicating that some aspects of gastrulation had occurred. At E8.5, apoptosis was more widespread than at E7.5 in $PTIP$-null mutants and its level was particularly high in the embryo proper (Fig. 3B and E). BrdU-positive cells were abundant in the wild-type embryos, representing about $52\% \pm 9\%$ of the total nuclei (Fig. 3F). In the $PTIP$-null mutants, BrdU-positive cells were only observed in regions that did not exhibit much apoptosis (Fig. 3C). Thus, $PTIP$ homozygous null embryos were smaller and disorganized because of an extremely high rate of cell death, starting in the embryonic ectoderm prior to gastrulation and continuing into later developmental stages.

To better examine the progression of $PTIP^{-/-}$ mutants through the cell cycle, we tried to isolate MEFs from E8.5. However, few cells from $PTIP^{-/-}$ embryos survived for more than a few days while wild-type embryo cells proliferated rapidly (data not shown). Even at earlier stages, blastocyst outgrowths from E3.5 showed clear inhibition of inner cell mass proliferation upon explant culture (Fig. 4). However, even in $PTIP$-null blastocysts, the trophoblast cells could spread out and adhere to the gelatinized plates. To test whether PTIP functions in the DNA damage pathways, we examined the sensitivity of $PTIP$ mutant trophoblast cells to ionizing radiation. After explantation, blastocysts were exposed to 2 Gy of ionizing radiation and allowed to recover for 7 days. The numbers of trophoblast cells adhering to the plates were scored (Table 1). At this dose, there was only an 18% reduction in the number of trophoblasts from wild-type or heterozygous blastocysts. However, $PTIP$-null cultures exhibited a 50% reduction in the number of viable trophoblast cells after 7 days in
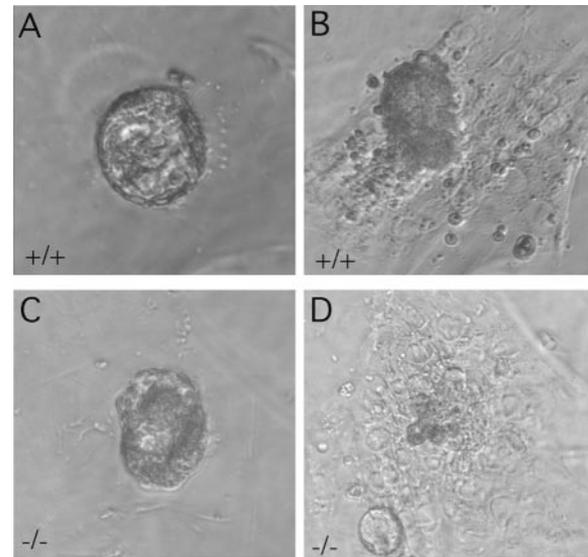

FIG. 4. Blastocyst outgrowth of wild-type (A, B) and $PTIP^{-/-}$ mutant (C, D) embryos. E3.5 embryos were flushed out of the uterine horns and cultured on collagen in DMEM–10% fetal calf serum. Phase-contrast micrographs were taken after 2 (A, C) or 5 (B, D) days in culture. In $PTIP^{-/-}$ mutants, trophoblast cells attach to the collagen matrix but very little inner cell mass was visible after 5 days.

culture. These data suggest an increased sensitivity of $PTIP$-null cells to low doses of ionizing radiation.

In the embryo proper, the cell cycle is rapid. Proteins known to function in the DNA damage pathways or cell cycle checkpoints in response to damage appear to be most essential in rapidly dividing cells of the inner cell mass and the embryonic ectoderm. To examine progression through the cell cycle in the embryo in more detail, serial sections from $PTIP$ mutants and age-matched littermates were immunostained with antibodies against α- and γ-tubulin and condensed chromatin was counterstained with $4',6'$-diamidino-2-phenylindole (DAPI) or propidium iodide (Fig. 5). While many $PTIP^{-/-}$ cells incorporated BrdU at E7.5, the number of cells with condensed chromatin was reduced at E7.5 and severely limited by E8.5. On average, approximately $2.5\% \pm 1\%$ of the cells of $PTIP$ mutants showed some condensed chromatin at E7.5 whereas $6.7\% \pm 0.8\%$ of the cells of wild-type embryos exhibited condensed chromatin. On histological sections, many cells in a wild-type E7.5 embryo could be seen in mitosis, as evidenced by segregating chromosomes, well-defined centrosomes, and an organized microtubular network (Fig. 5A and B). Although $PTIP^{-/-}$ mutants showed condensed chromatin, their chromosomes were not

TABLE 1. Effect of ionizing radiation on trophoblast proliferation in culture

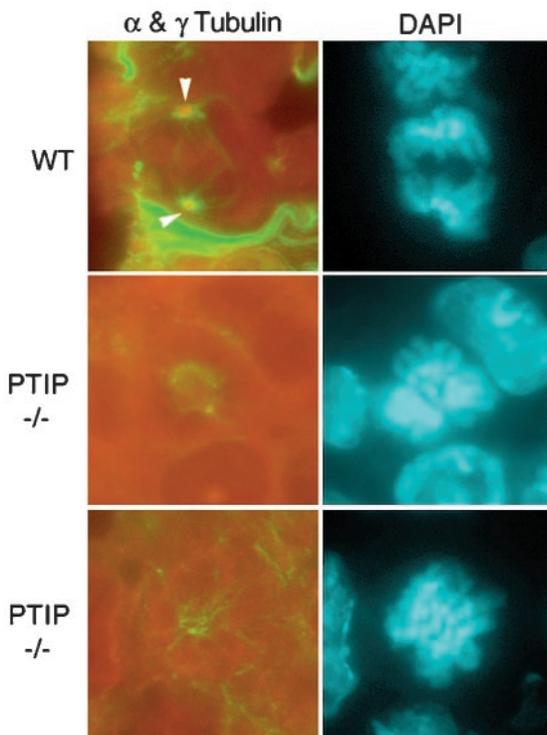| Genotype(s)	Mean proliferation $\pm$ 1 SD		% Reduction
	Untreated	2 Gy	
+/+, +/−	33.4 ± 9.9	27.5 ± 5.2^a	18
−/−	34.8 ± 5.9	17.6 ± 7.6^a	50

^{a} $P < 0.05$.

FIG. 5. Morphology of mitotic cells in wild-type (WT) and *PTIP*$^{-/-}$ mutant embryos. Paraffin sections (3 μm) from E7.5 embryos were immunostained with antibodies against α-tubulin (green) and γ-tubulin (red). The same image is shown counterstained with DAPI. Note the characteristic chromosomal segregation in the wild-type cell, the microtubular architecture (green), and the centrosomes (red, arrowheads). Centrosomes were undetected in *PTIP* mutants, the microtubules were poorly organized, and chromatin condensation appeared abnormal with little evidence of segregation.

well demarcated, few centrosomes were visible, and the microtubular network was poorly elaborated (Fig. 5C to F).

Phosphorylation of histone H3 is a hallmark of chromatin in mitosis and is necessary for cells to initiate chromatin condensation. Thus, we examined the status of histone H3 phosphorylation by immunocytochemistry and Western blotting (Fig. 6). Strikingly, at E8.5, *PTIP*$^{-/-}$ mutants exhibited very low levels of P-histone H3 while levels of acetylated-histone H3 remained unchanged (Fig. 6B). On sections of E8.5 littermates, P-histone H3 clearly demarcated condensed chromatin during mitosis in wild-type cells but stained poorly in *PTIP*$^{-/-}$ mutants (Fig. 6A). Both the number of mitotic cells and the intensity of staining for P-histone H3 were reduced in *PTIP*-null mutants. In *PTIP*-null mutants, approximately 2.4% ± 0.6% of the nuclei exhibited some positive staining for P-histone H3 whereas 7.8% ± 2.4% of the wild-type nuclei were P-histone H3 positive and generally showed greater intensity. Similar to the DNA dyes (Fig. 5), P-histone H3 staining revealed qualitative differences in condensed chromatin morphology between wild-type embryos and *PTIP*-null mutants. Mutant chromatin appears more globular, with little definition of individual chromosomes. By E9.5, very few P-histone H3-positive cells were present in mutant embryos, with only one or two faintly positive cells per section (data not shown). These data are consis-
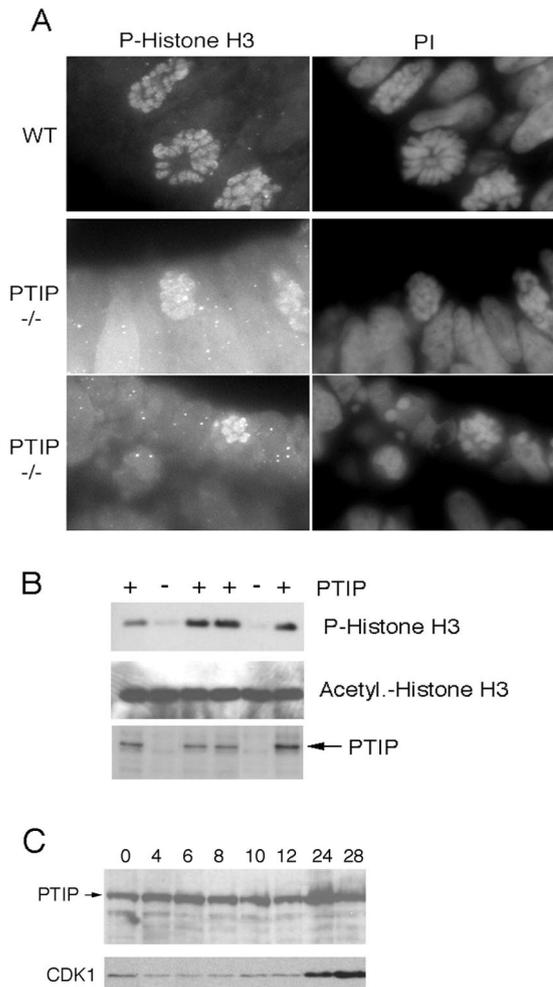

FIG. 6. Expression of P-histone H3 in wild-type (WT) and *PTIP*$^{-/-}$ mutant embryos. (A) Immunostaining for P-histone H3 and counterstaining with propidium iodide (PI) as indicated. Note that the low levels of P-histone H3 in *PTIP*$^{-/-}$ mutants does not demarcate the condensed chromatin very well. Also, the number of P-histone H3-positive cells was already reduced at E7.5 and very few remained by E8.5. (B) Western blot of total protein lysates from E8.5 showing a marked reduction of P-histone H3 but little effect on acetylated histone H3. The lysates were phenotyped by the presence or absence of PTIP (bottom). (C) Western blot of PTIP and phospho-CDK1 after addition of serum to starved MEFs. The time course of protein expression is indicated in hours after serum addition. Levels of PTIP did not vary significantly from quiescence to entry into mitosis.

tent with a failure to progress through the cell cycle from S phase to mitosis.

Given these observations, we examined the expression of *PTIP* during the cell cycle in culture (Fig. 6C). Primary MEFs were serum starved, activated with 20% serum, and examined for *PTIP* expression levels by Western blotting. No significant differences in *PTIP* expression levels were observed as cells entered the G$_2$/M transition, whereas phospho-CDK1 levels clearly increased beginning at 20 h postactivation.

DISCUSSION

By generating loss of a function allele, we have demonstrated an essential requirement for PTIP in early mouse de-

velopment. This requirement most likely reflects a need for PTIP in cell proliferation. To date, we have not found a cell or tissue type that fails to express PTIP, suggesting that it is an essential component of a common cellular process and not a tissue-specific transcription factor. The PTIP-null phenotype becomes clearly evident by E7.5 as significant cell death is detected, although DNA replication does not appear to be affected yet. However by E8.5, DNA replication is not evident in much of the embryo proper, as cell death is widespread.

Our analysis indicates that at E7.5, *PTIP* mutant cells are into and possibly through S phase and replicating DNA. In the TUNEL assay, significant amounts of free DNA ends are seen in *PTIP* mutants within the embryo proper at E7.5. While some apoptosis occurs in wild-type embryos, the labeled nuclei are generally pyknotic. Many *PTIP*-null nuclei are TUNEL positive even before nuclear condensation has occurred, suggesting that DNA breakage or failure to repair DNA strands may be an integral part of the null phenotype. Strikingly, cell death occurs first within the embryonic ectoderm, which generates the embryo proper. On the basis of BrdU labeling, the embryonic ectoderm proliferates more rapidly than the extraembryonic tissues and may thus be more sensitive to DNA damage. Perhaps because of the rapid rate of cell division, the embryonic ectoderm, prior to and at the time of gastrulation, appears to be particularly sensitive to mutations in the DNA damage checkpoint pathways. Mutations in the genes encoding the Chk1 kinase (16, 21) and its upstream activator, ATR (1, 4), lead to DNA damage and cell death by E7.5. As with our *PTIP* mutants, *ATR* and *Chk1* mutants also do not exhibit inner cell mass outgrowths when blastocysts are placed in culture. Complete *BRCA1*-null mutants (6, 15) have similar early lethal phenotypes at around E6.5, although embryos with deletions of just the BRCT domains of BRCA1 develop somewhat further to the head fold stage at E9.5 (8). The similarity of the *PTIP* and *Chk1*/*ATR* mutant phenotypes led us to examine whether *PTIP* mutants also fail to activate the G_2/M checkpoint upon UV irradiation. However, experiments with UV-irradiated blastocysts grown for 4 to 6 h in culture did not conclusively demonstrate a role for PTIP in checkpoint control at this stage (data not shown). *PTIP* mutant trophoblast cells did show increased sensitivity to ionizing radiation, similar to what has been observed for Brca2 (19) and the mouse *rad51* homologue (14). While these data are consistent with a role for PTIP in the damage control pathway, they do not allow us to assign a specific function.

Phosphorylation of histone H3 by the aurora-like kinases is essential for chromatin condensation and entry into mitosis (3, 9). Thus, the suppression of histone H3 phosphorylation observed in *PTIP* mutants can certainly prevent progression through mitosis. However, it is unclear whether this is a direct effect of loss of PTIP function or whether DNA damage or other upstream events result in the progressively lower levels of phospho-histone H3. Defects in heterochromatin condensation have also been observed in *Drosophila mus101* gene mutants (23), a multiple BRCT domain-encoding gene with some similarity to topoisomerase binding protein 1 (TopBP1), yeast Rad4/cut5, and mammalian PTIP. *mus101* mutants are also hypersensitive to DNA-damaging agents and exhibit genetic instabilities. The *PTIP*-null phenotype stands in contrast to that of mutants blocked from exit from mitosis, such as Sak

polo-like kinase mutants (10), in which more phospho-histone H3-positive cells accumulate. However, *Sak*-null mutants also show apoptosis and developmental arrest at the time of gastrulation. Thus, in *PTIP* mutants, mitotic arrest appears to occur at a stage in the cell cycle prior to that regulated by the Sak kinase. Our observations are consistent with a potential role for PTIP in the regulation of DNA repair, as has been reported for the yeast Crb2 protein. The BRCT domain protein Crb2 is necessary for topoisomerase III-mediated recombination repair in G_2 (2). Failure to initiate DNA repair can result in genetic instability, fragmented chromosomes, and cell death. If PTIP did function in DNA repair, one might predict its expression to be regulated during the cell cycle. We see no diminution of PTIP expression in quiescent cells or increased expression at S or G_2 phase. However, our experiments did not address the possibility of posttranslational modifications during the cell cycle.

The phenotype of *PTIP*-null mutants does not provide much insight into the potential for PTIP to mediate transcription regulation, as suggested by the interaction with Pax proteins and the binding of *Xenopus* Swift to Smad2. While the disorganized *PTIP* mutant E8.5 embryos vary greatly in the degree of differentiation, we can see neural tissue, head folds, and even somites in some embryos, suggesting that gastrulation can begin. We have also crossed the *PTIP*-null allele into *Smad2* mutants. A fraction of *Smad2* heterozygotes have gastrulation and other patterning defects (17). However, we have not observed any increase in developmental abnormalities in *Smad2*/*PTIP* double heterozygotes, although this negative result does not disprove an interaction.

While our data are suggestive of a role for PTIP in DNA repair, the potential for PTIP to function as a transcription activator through the conserved BRCT domains is not clear. Although the potential for PTIP to control elements of the cell cycle regulatory or DNA repair machinery at the transcriptional level is consistent with all of the data, it seems unlikely that PTIP functions as a tissue-specific activator during a time point in development, as most mutant embryos, while disorganized and developmentally retarded, do show evidence of gastrulation and differentiation. In summary, the mutant analysis presented in this report indicates that PTIP is likely to play an essential role in cell proliferation, perhaps as a component of the DNA damage/repair pathways. How mammalian PTIP functions at the biochemical level remains to be defined.

REFERENCES

1. **Brown, E. J., and D. Baltimore.** 2000. ATR disruption leads to chromosomal fragmentation and early embryonic lethality. Genes Dev. **14:**397–402.
2. **Caspari, T., J. M. Murray, and A. M. Carr.** 2002. Cdc2-cyclin B kinase activity links Crb2 and Rqh1-topoisomerase III. Genes Dev. **16:**1195–1208.
3. **Crosio, C., G. M. Fimia, R. Loury, M. Kimura, Y. Okano, H. Zhou, S. Sen, C. D. Allis, and P. Sassone-Corsi.** 2002. Mitotic phosphorylation of histone H3: spatio-temporal regulation by mammalian Aurora kinases. Mol. Cell. Biol. **22:**874–885.
4. **de Klein, A., M. Muijtjens, R. van Os, Y. Verhoeven, B. Smit, A. M. Carr,

A. R. Lehmann, and J. H. Hoeijmakers. 2000. Targeted disruption of the cell-cycle checkpoint gene ATR leads to early embryonic lethality in mice. Curr. Biol. **10:**479–482.

5. **Esashi, F., and M. Yanagida.** 1999. Cdc2 phosphorylation of Crb2 is required for reestablishing cell cycle progression after the damage checkpoint. Mol. Cell **4:**167–174.

6. **Hakem, R., J. L. de la Pompa, C. Sirard, R. Mo, M. Woo, A. Hakem, A. Wakeham, J. Potter, A. Reitmair, F. Billia, E. Firpo, C. C. Hui, J. Roberts, J. Rossant, and T. W. Mak.** 1996. The tumor suppressor gene Brca1. is required for embryonic cellular proliferation in the mouse. Cell **85:**1009–1023.

7. **Hoffmeister, A., A. Ropolo, S. Vasseur, G. V. Mallo, H. Bodeker, B. Ritz-Laser, G. R. Dressler, M. I. Vaccaro, J. C. Dagorn, S. Moreno, and J. L. Iovanna.** 2002. The HMG-I/Y-related protein p8 binds to p300 and Pax2 trans-activation domain-interacting protein to regulate the trans-activation activity of the Pax2A and Pax2B transcription factors on the glucagon gene promoter. J. Biol. Chem. **277:**22314–22319.

8. **Hohenstein, P., M. F. Kielman, C. Breukel, L. M. Bennett, R. Wiseman, P. Krimpenfort, C. Cornelisse, G. J. van Ommen, P. Devilee, and R. Fodde.** 2001. A targeted mouse Brca1 mutation removing the last BRCT repeat results in apoptosis and embryonic lethality at the headfold stage. Oncogene **20:**2544–2550.

9. **Hsu, J. Y., Z. W. Sun, X. Li, M. Reuben, K. Tatchell, D. K. Bishop, J. M. Grushcow, C. J. Brame, J. A. Caldwell, D. F. Hunt, R. Lin, M. M. Smith, and C. D. Allis.** 2000. Mitotic phosphorylation of histone H3 is governed by Ipl1/aurora kinase and Glc7/PP1 phosphatase in budding yeast and nematodes. Cell **102:**279–291.

10. **Hudson, J. W., A. Kozarova, P. Cheung, J. C. Macmillan, C. J. Swallow, J. C. Cross, and J. W. Dennis.** 2001. Late mitotic failure in mice lacking Sak, a polo-like kinase. Curr. Biol. **11:**441–446.

11. **Joyner, A. L.** 1993. Gene targeting: a practical approach. Oxford University Press, Oxford, United Kingdom.

12. **Koonin, E. V., S. F. Altschul, and P. Bork.** 1996. Functional motifs. Nat. Genet. **13:**266–268.

13. **Lechner, M. S., I. Levitan, and G. R. Dressler.** 2000. PTIP, a novel BRCT domain-containing protein, interacts with Pax2 and is associated with active chromatin. Nucleic Acids Res. **28:**2741–2751.

14. **Lim, D.-S., and P. Hasty.** 1996. A mutation in mouse *rad51* results in an early embryonic lethal that is suppressed by a mutation in *p53*. Mol. Cell. Biol. **16:**7133–7143.

15. **Liu, C. Y., A. Flesken-Nikitin, S. Li, Y. Zeng, and W. H. Lee.** 1996. Inactivation of the mouse Brca1 gene leads to failure in the morphogenesis of the egg cylinder in early postimplantation development. Genes Dev. **10:**1835–1843.

16. **Liu, Q., S. Guntuku, X. S. Cui, S. Matsuoka, D. Cortez, K. Tamai, G. Luo, S. Carattini-Rivera, F. DeMayo, A. Bradley, L. A. Donehower, and S. J. Elledge.** 2000. Chk1 is an essential kinase that is regulated by Atr and required for the G$_2$/M DNA damage checkpoint. Genes Dev. **14:**1448–1459.

17. **Nomura, M., and E. Li.** 1998. Smad2 role in mesoderm formation, left-right patterning and craniofacial development. Nature **393:**786–790.

18. **Saka, Y., F. Esashi, T. Matsusaka, S. Mochida, and M. Yanagida.** 1997. Damage and replication checkpoint control in fission yeast is ensured by interactions of Crb2, a protein with BRCT motif, with Cut5 and Chk1. Genes Dev. **11:**3387–3400.

19. **Sharan, S. K., M. Morimatsu, U. Albrecht, D. S. Lim, E. Regel, C. Dinh, A. Sands, G. Eichele, P. Hasty, and A. Bradley.** 1997. Embryonic lethality and radiation hypersensitivity mediated by Rad51 in mice lacking Brca2. Nature **386:**804–810.

20. **Shimizu, K., P.-Y. Bourillot, S. J. Nielsen, A. M. Zorn, and J. B. Gurdon.** 2001. Swift is a novel BRCT domain coactivator of Smad2 in transforming growth factor β signaling. Mol. Cell. Biol. **21:**3901–3912.

21. **Takai, H., K. Tominaga, N. Motoyama, Y. A. Minamishima, H. Nagahama, T. Tsukiyama, K. Ikeda, K. Nakayama, and M. Nakanishi.** 2000. Aberrant cell cycle checkpoint function and early embryonic death in Chk1$^{-/-}$ mice. Genes Dev. **14:**1439–1447.

22. **Welcsh, P. L., M. K. Lee, R. M. Gonzalez-Hernandez, D. J. Black, M. Mahadevappa, E. M. Swisher, J. A. Warrington, and M. C. King.** 2002. BRCA1 transcriptionally regulates genes involved in breast tumorigenesis. Proc. Natl. Acad. Sci. USA **99:**7560–7565.

23. **Yamamoto, R. R., J. M. Axton, Y. Yamamoto, R. D. Saunders, D. M. Glover, and D. S. Henderson.** 2000. The Drosophila mus101 gene, which links DNA repair, replication and condensation of heterochromatin in mitosis, encodes a protein with seven BRCA1 C terminus domains. Genetics **156:**711–721.

24. **Yarden, R. I., S. Pardo-Reoyo, M. Sgagias, K. H. Cowan, and L. C. Brody.** 2002. BRCA1 regulates the G$_2$/M checkpoint by activating Chk1 kinase upon DNA damage. Nat. Genet. **30:**285–289.